NJC

PAPER

Check for updates

Exothermal effects in the thermal decomposition of [IrCl$_6$]$^{2-}$-containing salts with [M(NH$_3$)$_5$Cl]$^{2+}$ cations: [M(NH$_3$)$_5$Cl][IrCl$_6$] (M = Co, Cr, Ru, Rh, Ir)†‡

S. A. Martynova,[ab] P. E. Plyusnin, [ID][ab] T. I. Asanova, [ID][a] I. P. Asanov,[a]
D. P. Pishchur, [ID][a] S. V. Korenev, [ID][ab] S. V. Kosheev,[c] S. Floquet,[d]
E. Cadot[d] and K. V. Yusenko [ID]*[ef]

[M(NH$_3$)$_5$Cl][IrCl$_6$], M = Co, Cr, Ru, Rh, and Ir, were proposed as single-source precursors for bimetallic alloys. Their thermal decomposition in inert and reductive atmospheres below 700 °C results in the formation of nanostructured porous Ir$_{0.5}$M$_{0.5}$ alloys. Salts decompose with a significant exothermal effect during the first stage of their thermal breakdown in an inert atmosphere above 200 °C. The exothermal effect gradually decreases in the series: [Co(NH$_3$)$_5$Cl][IrCl$_6$] (**1**) > [Cr(NH$_3$)$_5$Cl][IrCl$_6$] (**2**) > [Ru(NH$_3$)$_5$Cl][IrCl$_6$] (**3**) > [Rh(NH$_3$)$_5$Cl][IrCl$_6$] (**4**); [Ir(NH$_3$)$_5$Cl][IrCl$_6$] (**5**) does not exhibit any thermal effects and decomposes at much higher temperatures. To shed light on their thermal decomposition and the nature of the exothermal effect, DSC–EGA, *in situ* and *ex situ* IR, Raman, XPS and XAFS studies were performed. A combination of complementary techniques suggests a simultaneous ligand exchange and a reduction of central atoms as key processes. In [Co(NH$_3$)$_5$Cl][IrCl$_6$], Co(III) and Ir(IV) simultaneously oxidise coordinated ammonia, which can be detected due to a significant exothermal effect and the presence of Co(II) and Ir(III) in the intermediate product. The appearance of Ir–N frequencies demonstrates a ligand exchange between cations and the [IrCl$_6$]$^{2-}$ anion. Salts with Cr(III), Ru(III), and Rh(III) show a much lower exothermal effect due to the stability of their oxidation states. Salts with Rh(III) and Ir(III) demonstrate a high thermal stability and a low tendency for ligand exchange as well as decomposition with exothermal effects.

Introduction

Thermal stability and the decomposition of coordination compounds in the solid-state have been investigated since the development of thermal analysis. The most important early results were obtained by Wendlandt using thermal analysis coupled with other methods (mainly analysis of evolved gases (EGA), IR and electric conductivity) and were summarized in his book.[1] Nevertheless, the thermal properties of coordination compounds are still being investigated rigorously due to their importance for understanding reactivity in a solid state.

Detailed information about thermal stability and the reactivity of coordination compounds may lead to a better understanding of thermal-induced transformations and formation of various intermediate phases, which cannot be prepared in solution.[2] Various thermal-induced reactions can occur in the solid state such as ligand isomerisation (–NO$_2$ → –ONO), complex isomerisation (*cis-* → *trans-*), reduction and oxidation of the central atom *via* a ligand as well as complete degradation of coordination compounds with the formation of metallic or oxide nanostructured particles. In many cases, several parallel reactions occur simultaneously in a narrow temperature interval. As an example, double complex salts (DCSs) with coordination cations and coordination anions can undergo a simultaneous reduction of central atoms and ligand exchange when heated. Exothermic thermal transformation of [Cu(NH$_3$)$_4$][PtCl$_4$] in the solid state occurs at 190–200 °C without weight loss with the formation of isomeric [Pt(NH$_3$)$_4$][CuCl$_4$]. Such a complete ligand exchange between cations and anions is still a unique example in coordination chemistry.[3–5]

Octahedral cations and anions are more common in coordination chemistry and typical for Ir(III), Ir(IV), Rh(III), Co(II), Co(III), Cr(III), Pt(IV), and Pd(IV). Thermal decomposition

[a] Nikolaev Institute of Inorganic Chemistry, Lavrentiev ave. 3, 630090 Novosibirsk, Russia
[b] Novosibirsk State University, Pirogova str. 2, 630090 Novosibirsk, Russia
[c] Novosibirsk, Boreskov Institute of Catalysis, 630090 Novosibirsk, Russia
[d] Université de Versailles Saint-Quentin, Institut Lavoisier de Versailles (ILV), France
[e] College of Engineering, Swansea University, Fabian Way, Swansea SA1 8EN, Wales, UK. E-mail: k.yusenko@swansea.ac.uk
[f] Institute of Solid State Chemistry, Pervomaiskaia Str. 91, 620090 Ekaterinburg, Russia
† This paper is dedicated to the memory of Prof. Dr A. B. Venediktov (1948–2017) who recently passed away.
‡ Electronic supplementary information (ESI) available. See DOI: 10.1039/c7nj04035k

of coordination compounds with octahedrally coordinated transition metals is usually more complex due to the possibility for simultaneous reduction of the central atom by the coordinated ligand and at the same time the structural inaccessibility of the central atoms for a direct ligand exchange. As an example, the thermal decomposition of $[Pd(NH_3)_4][IrCl_6]$ occurs with an exothermic effect. Its decomposition was investigated in detail using TG, DSC–EGA supported by *ex situ* XPS and XAFS methods.[6,7] The authors proposed ligand exchange between cations and anions with a simultaneous reduction of Ir(IV) to Ir(III) by coordinated ammonia with the formation of N_2 as volatile product.

Previously, a representative series of double complex salts with a general formula $[M(NH_3)_5Cl][M'Hal_6]$ (M = Rh, Ru, Ir, Os, Cr, and Co; M' = Pt, Os, and Re, Ir; Hal = Cl, Br) weresynthesized and investigated structurally and by thermal analysis in inert (He, Ar, and N_2) and reducing (H_2) atmospheres below 700 °C.[8–10] Compounds were proposed as prospective single-source precursors for the preparation of bimetallic nanoporous alloys and supported catalysts under mild conditions.[11–13] Among others, a strong exothermal effect at 218–300 °C with a relatively small weight-loss (2–4 wt%) has been observed for salts with anionic Ir(IV), $[M(NH_3)_5Cl][IrCl_6]$ (M = Cr, Co, and Ru). After $[MA_4][MHal_4]$ and $[Pd(NH_3)_4][IrCl_6]$, $[M(NH_3)_5Cl][IrCl_6]$ salts represent a new series of bimetallic compounds with exothermal effects during thermal decomposition.

The $[M(NH_3)_5Cl][IrCl_6]$ series attracted special practical interest since all salts are isoformular and isostructural and crystallise from water solutions in the monoclinic $P2_1/m$ space group with close cell parameters (Fig. 1).[8–12] Their crystal structures consist of isolated $[M(NH_3)_5Cl]^{2+}$ cations and $[IrCl_6]^{2-}$ anions. Each cation has 6 anionic and each anion has 6 cationic neighbours similar to the NaCl structural type. The average M···M distances in their crystal structures are 5.7–5.7 Å. Co-crystallisation of individual salts results in the formation of mixed $[M'(NH_3)_5Cl]_x[M''(NH_3)_5Cl]_{1-x}[IrCl_6]$, which can be crystallized in the whole concentration interval and can be used for the preparation of alloys in a broad range of compositions.[14]

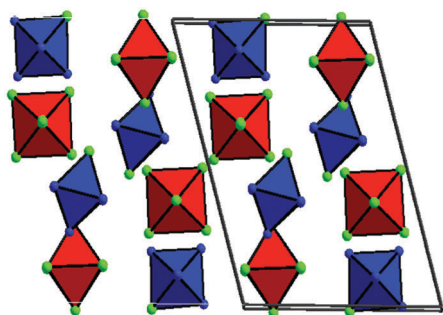Detailed investigation using a number of complementary techniques on a complete set of possible isostructural salts can shed light on very general tendencies in coordination chemistry. In the early days, thermal decomposition investigations were fragmented and based on thermal analysis and mainly *ex situ* IR or PXRD. The formation of complex intermediates and amorphous nanostructured phases usually caused many unsolved questions, which cannot be answered based only on a single technique. Nevertheless, a combination of thermal analysis and spectroscopy allows us to understand hidden and overlapping processes that occur when bimetallic salts are heated. Here, we report a systematic study of the thermal decomposition of $[Co(NH_3)_5Cl][IrCl_6]$ (**1**), $[Cr(NH_3)_5Cl][IrCl_6]$ (**2**), $[Ru(NH_3)_5Cl][IrCl_6]$ (**3**), $[Rh(NH_3)_5Cl][IrCl_6]$ (**4**), and $[Ir(NH_3)_5Cl][IrCl_6]$ (**5**) using TG, DSC–EGA supported by *in situ* and *ex situ* IR, Raman, XPS and XAFS techniques. Detailed investigation of mixed $[M'(NH_3)_5Cl]_x[M''(NH_3)_5Cl]_{1-x}[IrCl_6]$ with Co, Cr, Ru, Rh (with exothermic effect) and Ir (no exothermic effect) gives us a better understanding of the thermal properties of individual compounds as well as their thermodynamic properties.

Experimental

Compounds (**1**)–(**5**) were synthesized from aqueous solutions. Details can be found elsewhere.[9,14] Typically, aqueous solutions of $[M(NH_3)_5Cl]Cl_2$ (M = Cr, Co, Ru, Rh, and Ir) prepared according to the published procedures[9,15] were mixed with $(NH_4)_2[IrCl_6]$ aqueous solution at room temperature. After 10–15 minutes, fine brown precipitates were filtered, washed with 5–10 mL of ice-cold water, acetone and air dried. Yields were 85–95%. The addition of slight cation or anion excess might increase the yield of target salts. Mixed metal complexes were crystallized by mixing $[Ru(NH_3)_5Cl]Cl_2$ and $[Ir(NH_3)_5Cl]Cl_2$ with $(NH_4)_2[IrCl_6]$ aqueous solution.

The simultaneous TG-DSC/EGA-MS measurements were performed in an apparatus consisting of a STA 449 F1 Jupiter thermal analyser and an QMS 403D Aëolos quadrupole mass spectrometer (NETZSCH, Germany). The spectrometer was connected online to a thermal analyzer (STA) instrument by a quartz capillary heated to 280 °C. The measurements were made in a helium flow in the temperature range of 30–400 °C at a heating rate of 10 °C min⁻¹, at a gas flow rate of 30 mL min⁻¹ and using closed Al crucibles.

A DSC 204 F1 Phoenix (NETZSCH) equipped with a E-type thermocouple and a T-type heat flow sensor was used for precise differential scanning calorimetry experiments on powdered samples of 5–10 mg. Precise DSC experiments were performed to estimate a specific heat change during the exothermal reaction.

The IR-spectra of starting compounds and intermediates were collected *ex situ* using a Scimitar FTS 2000 Fourier-spectrometer "DIGILAB" (4000–400 cm⁻¹ region) and a Vertex 80 "Bruker" spectrometer (600–100 cm⁻¹ region). Samples were heated in helium and pressed with dry KBr or polyethylene, correspondingly.

The variable temperature (*in situ*) FT-IR spectra were recorded on an IRTF Nicolet iS10 spectrometer in diffuse reflectance mode by using a high-temperature diffuse reflectance environmental chamber. The background was recorded on dry KBr at 150 °C.

Fig. 1 Crystal structure of $[Ru(NH_3)_5Cl][IrCl_6]$ (**3**) along the monoclinic axis y: a = 11.726(2) Å, b = 8.333(2) Å, c = 15.755(3) Å, β = 105.13(3)°, V = 1577.5 Å^3, $P2_1/m$, Z = 4. $[Cr(NH_3)_5Cl]^{2+}$ cations are shown in red, $[IrCl_6]^{2-}$ anions and N – in blue, green – Cl; hydrogen atoms are omitted for clarity.

The samples were diluted with 90 wt% of KBr. The FT-IR spectra were recorded in the 20–580 °C temperature range under nitrogen flow using a heating rate of 2 K min^{-1}. The spectra were recorded with a resolution of 0.4 cm^{-1}.

The Raman spectra were recorded using a LabRAM HR, Horiba spectrometer with an Ar laser CVI Melles Griot (λ 633 nm). Spectra were collected in reflection mode under a Raman microscope with a 0.5 cm^{-1} resolution. All compounds with Ir(IV)–Cl bonds show resonance with a 633 nm laser beam which results in a high intensity of the corresponding frequency.[16]

The XAFS spectra were collected at the 10C beam-line at PAL (Pohang Accelerator Laboratory, Republic of Korea). The ring current was about 100 mA at 2.0 GeV. A Si(111) double crystal was used as a monochromator. [M(NH$_3$)$_5$Cl][IrCl$_6$] (M = Co, Ru, Cr, Ir, and Rh) were ground with h-BN in an agate mortar and pressed into pellets. For each *ex situ* XAFS experiment at the Co, Cr or Ir edges, individual pellets were used. Pellets were placed in a custom furnace and heated in N$_2$ flow. Temperature was controlled with a PX Series Hanyoung Electronic Co., Ltd. Data were recorded using three ionization detectors measuring the beam intensity of incidence (I_0), transmitted through the sample (I_t) and transmitted through the reference (I_{ref}). The reference channel was employed primarily for the internal calibration of the edge positions using pure metal foils. All chambers were filled with nitrogen. XAFS data were analysed using IFFEFIT software.[17]

X-ray photoelectron spectra (XPS) of [Ir(NH$_3$)$_5$Cl][IrCl$_6$] and its intermediate product heated up to 370 °C (just after the first exothermic effect on the DSC curve with a weight loss about 7 wt%) were recorded on a KRATOS ES-300 (Kratos Analytical, UK) under 10–12 bars of pressure with a Mg anode ($h\nu$ = 1253.6 eV). Spectra were fitted using GL-doublets.

Results

Thermal analysis

(**1**), (**2**) and (**3**) show a pronounced exothermic effect (Fig. 2 and Table 1) accompanied by a slight weight-loss. The first exothermic effect partially overlapped with a further endothermic process especially in (**1**). A strong overlapping and change of the base line after decomposition makes it impossible to obtain precise measurements of temperature, enthalpy, and weight-loss for all compounds including mixed salts [M'(NH$_3$)$_5$Cl]$_x$[M''(NH$_3$)$_5$Cl]$_{1-x}$[IrCl$_6$]. As a result, parameters were estimated using the horizontal baseline approximation.

(**4**) shows no evidence of exothermal effects. Nevertheless, a sensitive DSC shows two overlapping simultaneous thermal processes, which can be associated with the oxidation state change (exothermal reaction) and the ligand exchange (endothermal reaction). Upon heating, slight energy release (*ca.* −3.2 kJ mol^{-1}) was detected. Nevertheless, a simultaneous endothermic process completely masks the process. The endothermic process (*ca.* +58.8 kJ mol^{-1}) has two visible maxima, which can be associated with two temperature-isolated ligand-exchanges. 31% of heat corresponds to the first peak and 69% to the second.
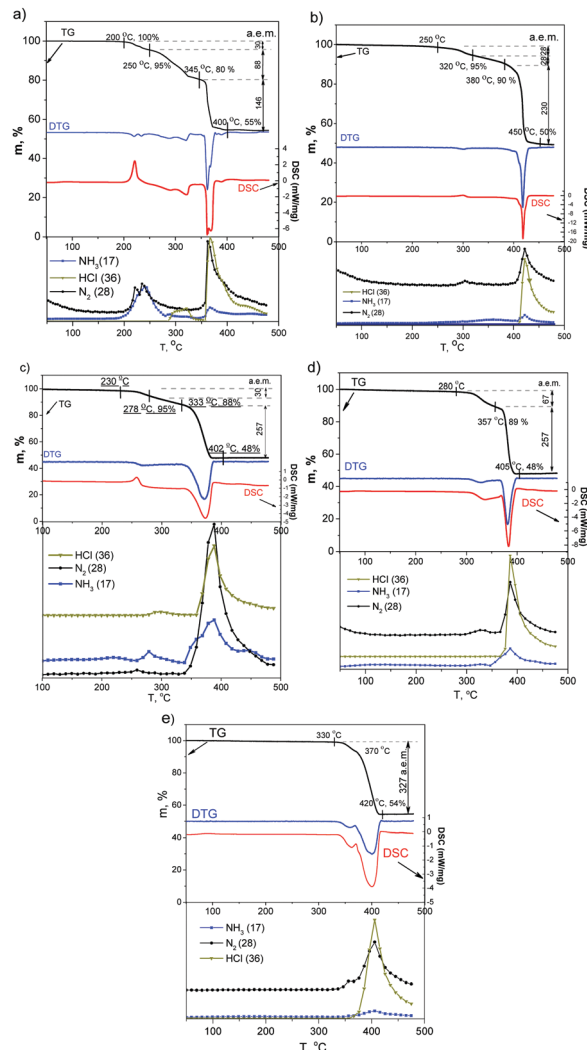

Fig. 2 TG, DTG, DSC and EGA curves of [M(NH$_3$)$_5$Cl][IrCl$_6$] (He flow, heating rate 10 K min^{-1}): (a) (**1**), (b) (**2**), (c) (**3**), (d) (**4**), (e) (**5**).

Table 1 DSC data for exothermal effects in [M(NH$_3$)$_5$Cl][IrCl$_6$]

Compound	T_{Onset}, °C	ΔH, kJ mol^{-1}	Δm, % (a.e.m.)
(**1**)	200	−135.50	2.00 (11.64)
			4.37 (25.43)
(**2**)	250	−52.75	5.04 (28.98)
(**3**)	230	−22.25	5.20 (32.50)
[Ru$_{0.90}$Ir$_{0.10}$(NH$_3$)$_5$Cl][IrCl$_6$]	245	−7.63	2.96 (18.49)
[Ru$_{0.66}$Ir$_{0.34}$(NH$_3$)$_5$Cl][IrCl$_6$]	250	−2.95	4.74 (29.61)
[Ru$_{0.50}$Ir$_{0.50}$(NH$_3$)$_5$Cl][IrCl$_6$]	270	−0.50	4.72 (29.49)
(**4**)	280	−3.27	10.70 (66.98)

(**5**) with (Ir(III) in cation and Ir(IV) in anion) does not show any detectable exothermic processes. As a result, its thermal decomposition starts at a slightly higher temperature (above 300 °C) and can be associated with two non-resolved endothermic effects.

The DTG curve of (**1**) (Fig. 2) suggests 5 decomposition stages in the 200–400 °C interval. The first weight-loss step (*ca.* 5 wt%) at 200–250 °C corresponds to an exothermic process detected on the DSC curve (max at ∼220 °C). According to EGA,

the compound releases gases with m/z = 14, 28 (N_2), 15, 16 and 17 a.e.m. (NH_3). Further two high-temperature steps (250–345 °C) with total weight-loss of about 15 wt% partially overlap with the first exothermic process. EGA curves suggest release of HCl (m/z = 35, 36, 37 and 38 a.e.m.). The last step at 345–400 °C corresponds to 25 wt% weight-loss and release of gases with m/z = 14, 28 (N_2), 36, 38, 35, 37 (HCl) and a small amount of NH_3 (m/z = 15, 16 and 17 a.e.m.).
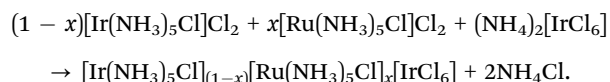
(**3**) (Fig. 1) decomposes at 230–402 °C with only two stages on the DTG curve. The first stage at 230–278 °C corresponds to weight loss of 5 wt% and the exothermic effect (at 260 °C). The compound releases only N_2 (m/z = 14 and 28 a.e.m.). The second stage at 278–333 °C corresponds to the release of HCl (m/z = 36, 38, 35 and 37 a.e.m.) and NH_3 (m/z = 17, 16 and 15 a.e.m.) without any significant changes in its DTG curve, which can be associated with a sublimation of NH_4Cl. Later at 333–400 °C, the sample loses *ca.* 40 wt% which corresponds to a release of N_2, HCl and NH_3.

(**2**) decomposes in a way very similar to (**3**) (Fig. 2).

According to TG and DTG curves (Fig. 2), thermal decomposition of (**4**) is a two stage process. Nevertheless, the DSC profile of the first stage is more complex than other isoformular complexes (Fig. 3). The slightly exothermic effect overlaps with a following endothermic process. The endothermic process can be divided into a minimum of two stages, which can be associated with a step-by-step ligand exchange. Salt loses *ca.* 11 wt% at 280–357 °C with the release of N_2 (m/z = 14 and 28 a.e.m.), NH_3 (m/z = 15, 16 and 17 a.e.m.) and HCl (m/z = 35, 36, 37 and 38 a.e.m.). Further heating (357–405 °C) corresponds to 41% weight-loss with the release of N_2, NH_3, HCl.

(**5**) salt has only two overlapping endothermic peaks (300–420 °C) with a total weight loss of 52 wt%. At the beginning, only a slight release of N_2 can be detected. Further heating corresponds to the evolving of N_2, NH_3, HCl. Thermal analysis information is summarized in Table 1.

The first exothermal effect is unique and depends on the metal cation. The effect is characteristic not only for individual salts $[M(NH_3)_5Cl][IrCl_6]$ but also for mixed salts such as $[Ru_xIr_{1-x}(NH_3)_5Cl][IrCl_6]$. $[M(NH_3)_5Cl]$ salts are isoformular and isostructural with close cell parameters. Co-crystallisation from solutions containing two cations or two anion results in the formation of multimetallic salts.[9,18] Co-crystallisation of $[Ru_xIr_{1-x}(NH_3)_5Cl][IrCl_6]$ salts with $[Ru(NH_3)_5Cl]^{2+}$ (clear exothermic effect) and $[Ir(NH_3)_5Cl]^{2+}$ (no endothermal effect) can be summarised as follows:

$$(1 - x)[Ir(NH_3)_5Cl]Cl_2 + x[Ru(NH_3)_5Cl]Cl_2 + (NH_4)_2[IrCl_6]$$
$$\rightarrow [Ir(NH_3)_5Cl]_{(1-x)}[Ru(NH_3)_5Cl]_x[IrCl_6] + 2NH_4Cl.$$

Synthesis is reproducible and can be used for the preparation of multicomponent alloys in a broad range of compositions. A gradual change in the composition results in a gradual change in the thermal properties of mixed salts (Table 1). Salts with a high Ru content show a pronounced exothermal effect. Nevertheless, already $[Ru_{0.5}Ir_{0.5}(NH_3)_5Cl][IrCl_6]$ can be characterized by a negligible exothermic effect similar to (**5**).
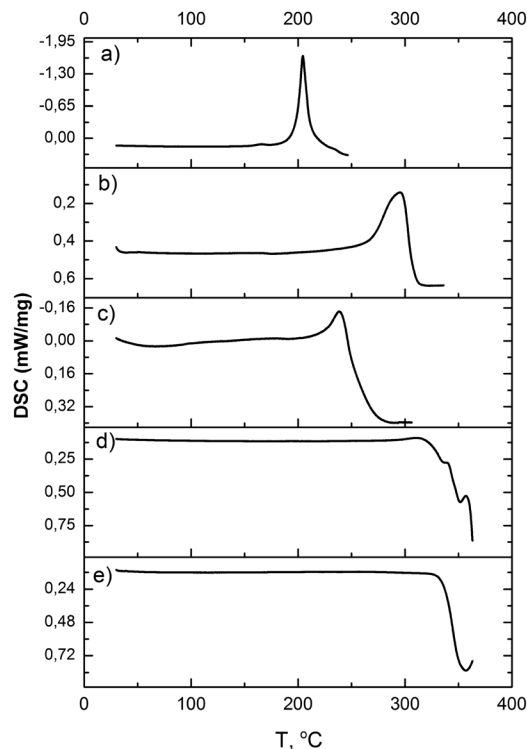

Fig. 3 DSC curves of $[M(NH_3)_5Cl][IrCl_6]$ (Ar flow, 6 K min^{-1}): (a) (**1**), (b) (**2**), (c) (**3**), (d) (**4**), (e) (**5**).

FT-IR and Raman study

Intermediates prepared at various temperatures in helium flow were quenched to room temperature and investigated *ex situ* using IR and Raman spectroscopy to clarify bonding in double complex salts before and after exothermal reactions. Complementary IR and Raman spectroscopic data were collected *ex situ* in the 80–600 cm^{-1} range (Fig. 3 and Table S1, ESI‡). Additionally, *in situ* and *ex situ* IR data (400–4000 cm^{-1}) were collected to support fare-region studies (Fig. 4 and Table S1, ESI‡).

The Raman spectra of (**1**) contain intense frequency at 346 cm^{-1} corresponding to a valence Ir(IV)–Cl vibration similar to one at 352 cm^{-1} characteristic of $K_2[IrCl_6]$. A Raman resonance with a 633 cm^{-1} laser beam results in an increased intensity of the corresponding line. A small shoulder at 326 cm^{-1} can be associated with a valence Co(III)–Cl frequency. A frequency at 478 cm^{-1} of low intensity corresponds to Co(III)–N valence vibrations.[16,17,19,20]

Above 210 °C, intensities of Ir(IV)–Cl and Co(III)–N frequencies decrease with the appearance of an asymmetric line at 315 cm^{-1} with a shoulder at 295 cm^{-1} which can be associated with Co(II)–Cl and Ir(III)–Cl, respectively. Above 240 °C (the middle part of exothermic effect), Ir(IV)–Cl vibrations were not detected. Simultaneously, frequency at 315 cm^{-1} grows in intensity. Frequencies corresponding to M–N valence vibrations shift from 483 (dominant Co(III)–N) to 513 cm^{-1} (dominant Ir(III)–N, similar to $[Ir(NH_3)_5Cl]Cl_2$), which can be explained as NH_3-ligand exchange between Co and Ir. Above 300 °C, only frequencies at 519 (Ir(III)–N) and 317 cm^{-1} (Co(II)–Cl) were detected.
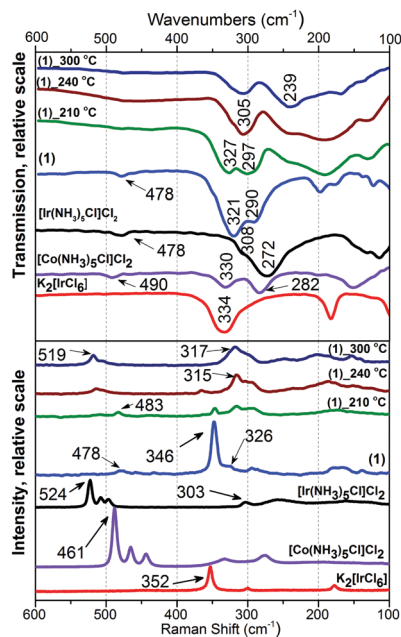
Fig. 4 IR (above) and Raman (below) spectra of (**1**).

Fig. 5 *In situ* experiments of (a) (**3**) and (b) (**2**) under a N_2 atmosphere.

The most informative line in the near IR-spectra of all compounds corresponds to $\rho_r(NH_3)$ (rocking mode) and $\nu(M-N)$ (Table S1, ESI‡). For (**1**) both lines are sensitive to the M–N bond-length and the nature of the metal. Above 210 °C, $\rho_r(NH_3)$ frequencies shift to a shorter wavelength of 28 cm^{-1}, which corresponds to Ir(III)–N frequency.

A frequency at 321 cm^{-1} in the IR-spectra of (**1**) can be associated with Ir(IV)–Cl valence vibrations (Fig. 3). It shifts to shorter wavelengths above 210 °C depicting the formation of Co(III)–Cl bonds. Above 240 °C, vibrations shift to higher wavelengths, which corresponds to the decrease of charge on central atoms due to Co(III) to Co(II) and Ir(IV) to Ir(III) reduction. In the IR middle-range spectra (*ex situ* data) above 210 °C, a 1400 cm^{-1} frequency corresponds to deformation vibrations of NH_4^+.

In the Raman spectra of (**2**) (Fig. S1, ESI‡), the frequency at 348 cm^{-1} (Ir(IV)–Cl) disappears with heating and the shoulder at 321 cm^{-1} (Cr(III)–Cl) shifts to 315 cm^{-1}. M–N frequencies in the Raman spectra of $[Cr(NH_3)_5Cl][IrCl_6]$ were not detected. Nevertheless, above 280 °C, the strong new line at 518 cm^{-1} can be attributed to Ir(III)–N bonds. In the IR-spectra of (**2**), intensity at 320 cm^{-1} (M–Cl) decreases with heating and shifts to longer wavelengths which corresponds to Cr(III)–Cl and Ir(III)–Cl bonds.

IR and Raman spectra of (**3**) (Fig. S2, ESI‡) change with heating similarly to (**2**). Frequency at 482 cm^{-1} (Ru–N) significantly shifts to 504 cm^{-1}, which also corresponds to the formation of Ir(III)–N bonds.

(**4**) and (**5**) do not show any significant changes in their IR and Raman spectra. Nevertheless, according to DSC, their thermal decomposition is similar to the other isoformular compounds discussed above.

In situ and *ex situ* middle-range region IR spectra collected for (**2**) and (**3**) do not show any visible differences (Fig. 5). Lines corresponding to 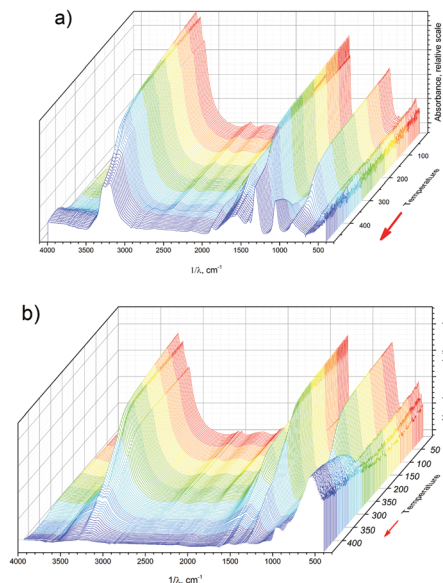the valence frequencies of NH_4^+ (1400–1405 cm^{-1}) are much higher in intensity in *ex situ* experiments in comparison with *in situ* data. Strong lines at 1070 and 528 cm^{-1} can be associated with Ru=O and Cr–O valence vibrations, respectively, and can be explained by partial air oxidation of intermediate products collected *ex situ* after quenching from various temperatures in He. Small lines corresponding to oxygen containing species in *in situ* spectra can be due to impurities in N_2 gas and possible contamination of *in situ* equipment, which nevertheless do not alter the process of salt decomposition.

XPS and EXAFS techniques

Ir4f, Cl2p and N1s XPS lines of (**5**) were scanned twice in 25 min. to check time and radiation stability. As a result, a slight charge shift to the higher energies has been detected for the second measurement. The starting double salt shows a smaller charge shift. Radiation damage is associated with N and Cl ligand-loss (Table S2, ESI‡). The starting salt can be characterized by double sets of spectroscopic lines for all elements (Fig. 6). The intermediate product with 7 wt% weight-loss prepared at 370 °C does not show doublets and has a single set of spectroscopic lines with asymmetric profiles, which can be associated with nonisotropic surface charge. The Ir4f spectra (Fig. 6a and d) of the intermediate suggest nearly complete Ir(IV) to Ir(III) reduction. The initial salt has a higher energy of Ir–Cl (63.4–63.6 eV) than the the Ir–N bond (E = 62.0–62.4 eV). Starting $[Ir(NH_3)_5Cl][IrCl_6]$ has two components with a 4:1 ratio corresponding to N–Ir–N and N–Ir–Cl in its nitrogen spectra. After thermal decomposition, Ir(IV) was not detected, and N and Cl spectra show only single components. Residual surface bonded NH_3 was detected as the second component in the N1s spectra (E = 398.6 eV). The intermediate has only a single chlorine component with E = 198.8 eV.

The XANES spectra at Ir-L_3, Co-K and Cr-K edges measured *ex situ* for initial (**1**), (**2**), (**3**) and intermediate products and corresponding Fourier transformed k^2-weighted EXAFS are
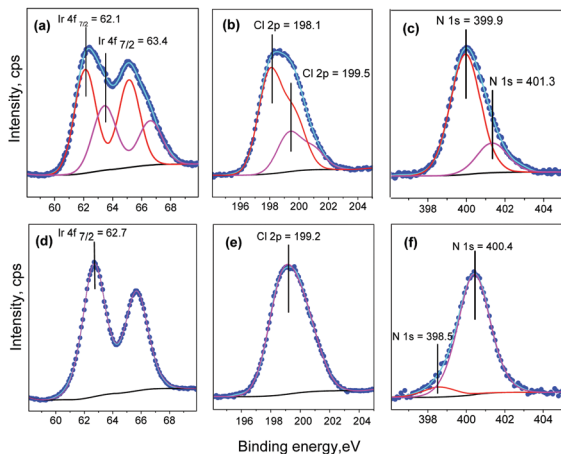
Fig. 6 XPS spectral decomposition (**5**) on individual GL-components: the initial salt (a–c) and decomposition intermediate 370 °C (d–f).

summarized in Fig. 7–9. All initial salts are isoformular and isostructural with identical coordination of Ir(IV) and as a result have identical Ir-L₃ XANES spectra.

For (**1**), EXAFS analysis suggests an increasing Ir–Cl bond length in intermediate products. The coordination sphere of Ir is equal to 6 Cl-ligands in the starting salt and 3.9–4.5 N atoms and 1.2–1.8 Cl in intermediates (Table 2). It is important that coordination numbers are equal for both intermediates investigated in preparations at 215 and 239 °C.

Cobalt in both its typical oxidation states, Co(II) and Co(III), has been reported to have a number of characteristic features in the XANES spectra, which can be used to qualify and quantify the oxidation state.[17,21] The Co(III) spectra usually show two
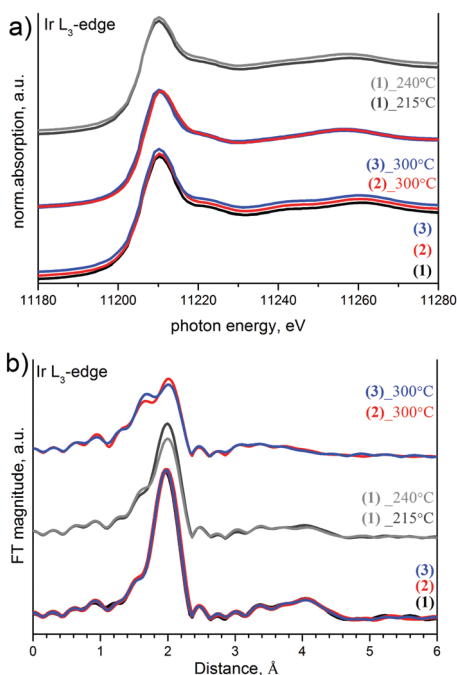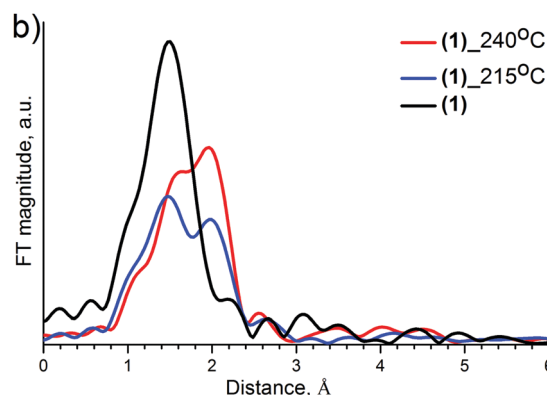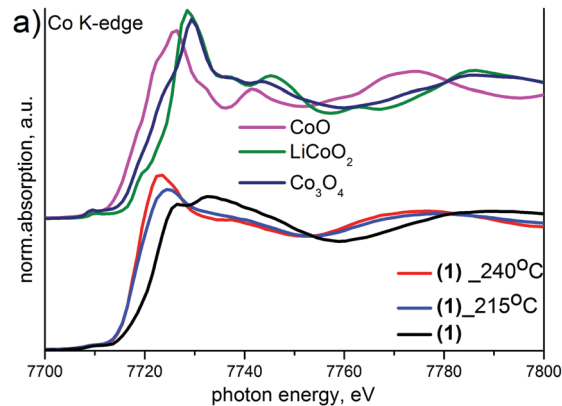

Fig. 8 Co K-edge XANES (a) and Fourier transformed k^2-weighted EXAFS (b) of (**1**).

absorption edge peaks at around 7727 and 7736 eV associated with two components of 1s to 4p transition. Many Co(III) complexes but no Co(II) species show a small pre-edge peak at about 7709 eV associated with a 1s → 3d transition. The XANES spectra of Co(II) show only a single absorption peak at 7723 eV and typically of about 1.5 eV lower than the edge observed for most Co(III) complexes.[22–24] Initial (**1**) shows two maxima with a pre-edge peak typical for Co(III) species (Fig. 8). Intermediates measured after heating contain Co(II) while their single maxima shifted to lower energy without a pre-edge feature. The intermediate obtained at 240 °C contains more Co(II) than an intermediate quenched from 215 °C, which contains a mixture of Co(II) and Co(III).

It is also likely that Ir has been reduced from Ir⁴⁺ to Ir³⁺ simultaneously with a ligand exchange and Co³⁺ to Co²⁺ reduction. The iridium oxidation state can be detected by a shift of the edge maximum to the lower energies.

Similarities in the XAFS spectra of (**2**) and (**3**) heated to 300 °C correspond to similarities in their decomposition process. Ir effective coordination spheres for Ir are ∼3.6(4) N and 2.4(4) Cl in both salts due to ligand exchange. The Cr-K edge does not visibly change upon heating (Fig. 9), which suggests a stability of Cr(III) with 4 nitrogen atoms and 2 chlorines in a Cr coordination sphere. Nevertheless, the line shape changes significantly, which indicates significant changes in geometry before and after heating due to a decrease in the coordination number and Cl to N substitution.
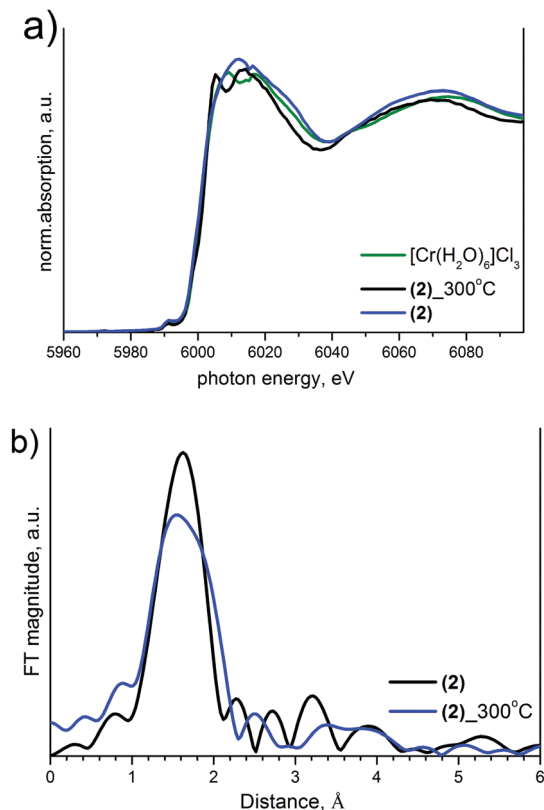

Fig. 7 Ir L₃-edge XANES (a) and Fourier transformed k^2-weighted EXAFS (b) of initial salts and intermediate products.

Fig. 9 Cr K-edge XANES (a) and Fourier transformed k^2-weighted EXAFS (b) of (**2**).

Table 2 EXAFS data for (**1**), (**2**), (**3**) and intermediate products quenched after heating in helium

Sample	Edge	Bond	r, Å	σ^2, Å^2	N	R
(**1**)	Ir L$_3$	Ir–Cl	2.331(6)	0.0026(4)	6	0.012
Intermediate, 215 °C	Ir L$_3$	Ir–N	2.042(3)	0.003(1)	4.5(3)	0.008
		Ir–Cl	2.357(4)	0.0022(3)	1.2(2)	—
	Co K	Co–N	1.977(9)	0.006(1)	2.7(3)	0.003
		Co–Cl	2.230(9)	0.016(1)	3.3(3)	—
Intermediate, 240 °C	Ir L$_3$	Ir–N	2.046(4)	0.0025(9)	3.9(3)	—
		Ir–Cl	2.360(5)	0.0022(3)	1.8(2)	—
	Co K	Co–N	2.085(9)	0.005(1)	2.3(8)	0.005
		Co–Cl	2.459(9)	0.009(1)	3.7(8)	—
(**2**)	Ir L$_3$	Ir–Cl	2.338(5)	0.0025(3)	6	0.01
	Cr K	Cr–N	2.103(9)	0.001(1)	5	0.02
		Cr–Cl	2.33(2)	0.002(1)	1	—
Intermediate, 300 °C	Ir L$_3$	Ir–N	2.076(7)	0.0022(9)	3.6(4)	0.01
		Ir–Cl	2.363(7)	0.0018(9)	2.4(4)	—
	Cr K	Cr–N	2.020(9)	0.004(1)	4	0.01
		Cr–Cl	2.352(8)	0.004(1)	2	—
(**3**)	Ir L$_3$	Ir–Cl	2.338(5)	0.0025(3)	6	0.01
Intermediate, 300 °C	Ir L$_3$	Ir–N	2.079(6)	0.003(1)	3.6(4)	—
	Ir L$_3$	Ir–Cl	2.366(7)	0.0012(5)	2.4(4)	—

Ru-K edge investigation has not been performed to prove ligand migration from the Ru site. The XANES Ir L$_3$ spectra show a significant decrease in the integral intensity of the white line reflecting a density of unoccupied states, which corresponds to a decrease in the Ir oxidation state. In other words, XANES data

confirm a reduction from Ir(IV) to Ir(III) in parallel to the ligand exchange. Ir coordination and interatomic bonds in intermediate products are similar for Cr and Ru compounds. In both cases, the structure of Cr and Ru intermediates should be similar to each other and different from Co-containing species.

Discussion

Double complex salts with $[IrCl_6]^{2-}$ anions and $[M(NH_3)_5Cl]^{2+}$ or $[M(NH_3)_4]^{2+}$ can be used as single-source precursors for bimetallic and multicomponent nanoporous alloys.[6,13,25–28] Their thermal decomposition in an inert or a reductive atmosphere occurs below 700 °C. An important feature of their thermal behaviour is a significantly large exothermal effect at the early decomposition stage (below 150–200 °C). Five isoformular and isostructural salts $[M(NH_3)_5Cl][IrCl_6]$ exhibit a promising model system where exothermal effects gradually decrease in the series: (**1**) > (**2**) > (**3**) > (**4**).

The exothermic effect in (**1**) was estimated to be −135.50 kJ mol^{-1}, which is 2.5 times higher than (**2**) and 11 times higher than (**3**). The high exothermic effect in (**1**) can be associated with a simultaneous reduction of Co(III) to Co(II) and Ir(IV) to Ir(III). (**2**) and (**3**) show strong overlapping of two reactions as well as a decrease in heat capacity after the first step, which can be associated with the formation of more complex polymeric structures. At the same time, the formation of Cr(II) and Ru(II) species was not detected.
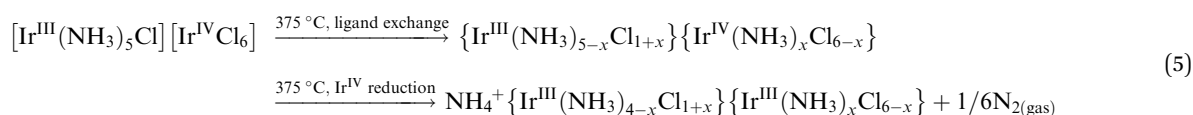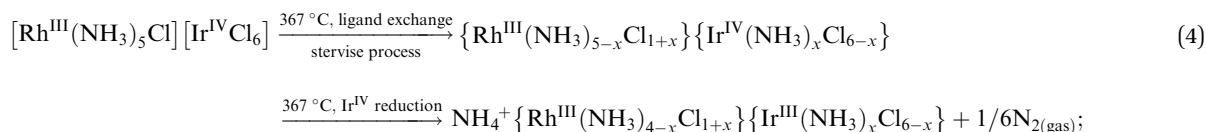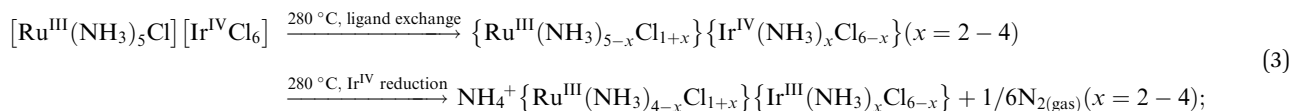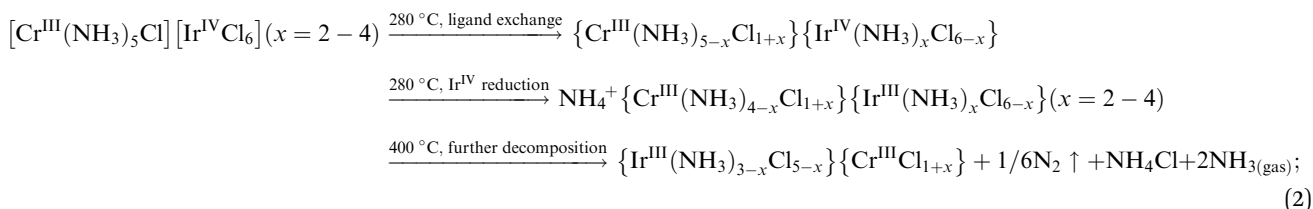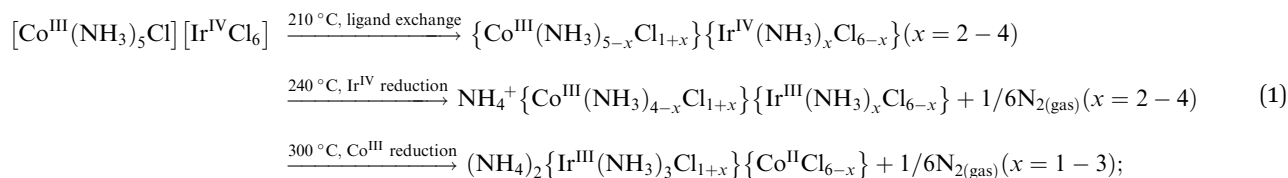
Corresponding weight-loss can be associated with the release of N$_2$. Nitrogen only occurs as a product of NH$_3$ oxidation and suggests that in general a reduction of metals by coordinated ammonia is the main pathway of the thermal degradation of $[M(NH_3)_5Cl][IrCl_6]$ compounds in an inert atmosphere. A combination of IR, Raman, XPS and EXAFS data gives more detailed insights into the processes, which result in the exothermic effect. There are three main processes which correspond to the decomposition in inert gas flow: (i) ligand exchange between cations and anions; (ii) reduction of Ir(IV) to Ir(III); and (iii) reduction of cationic M(III) to M(II), which occurs only in Co-containing species.

N$_2$ release as well as the presence of Ir(III) species after the first stage were detected in all five salts. Nevertheless, M(III) to M(II) reduction was detected only for (**1**) while Co(III) also shows a high tendency for reduction in the solid-state and in solution. Intermediate (**1**) shows the presence of only Co(II) and Ir(III).

Frequencies in the Raman and IR-spectra characteristic of Ir(III)–Cl, Ir(III)–N as well as of M–Cl and M–N can be detected in intermediate products and prove a ligand exchange between cations and anions. The presence of M═O and M–O valence frequencies detected in quenched samples investigated *ex situ* and *in situ* can be associated with partial air oxidation of highly reactive intermediates. The presence of (NH$_4$)$^+$ rotations detected in quenched samples investigated *ex situ* using IR and Raman can be associated with crystallisation and further degradation of intermediates, while the *in situ* IR-spectra do not contain a significant amount of (NH$_4$)$^+$ species.

The higher content of NH_4^+-containing intermediates in the spectra collected *ex situ* might be a general tendency corresponding to post-decomposition air-, water- or time-degradation of reactive intermediates and not specific for thermal decomposition of double complex salts themselves. It might be important to revise the existing experimental data for ammonia-containing coordination compounds investigated *ex situ*. Some important bright and visible features might be due to the sample degradation and can be considered as possible artefacts after careful *in situ* investigation. Schematically, decomposition processes can be summarized as follows:

migrated to the Ir(III) centre. Thermal decomposition is a process strictly regulated by the chemical nature of opposite cations. In the case of less stable Co(III), the reaction occurs at low temperature with a pronounced exothermic effect. More stable Ir(III) and Rh(III) do not decompose with visible thermal effects and reveal high thermal stability.

Conclusions

Thermal decomposition of isoformular salts $[M(NH_3)_5Cl][IrCl_6]$ exhibits exothermal effects below 200 °C. The value of the effect

$$[Co^{III}(NH_3)_5Cl][Ir^{IV}Cl_6] \xrightarrow{210\ °C,\ ligand\ exchange} \{Co^{III}(NH_3)_{5-x}Cl_{1+x}\}\{Ir^{IV}(NH_3)_xCl_{6-x}\}(x = 2-4)$$

$$\xrightarrow{240\ °C,\ Ir^{IV}\ reduction} NH_4^+\{Co^{III}(NH_3)_{4-x}Cl_{1+x}\}\{Ir^{III}(NH_3)_xCl_{6-x}\} + 1/6N_{2(gas)}(x = 2-4) \quad (1)$$

$$\xrightarrow{300\ °C,\ Co^{III}\ reduction} (NH_4)_2\{Ir^{III}(NH_3)_3Cl_{1+x}\}\{Co^{II}Cl_{6-x}\} + 1/6N_{2(gas)}(x = 1-3);$$

$$[Cr^{III}(NH_3)_5Cl][Ir^{IV}Cl_6](x = 2-4) \xrightarrow{280\ °C,\ ligand\ exchange} \{Cr^{III}(NH_3)_{5-x}Cl_{1+x}\}\{Ir^{IV}(NH_3)_xCl_{6-x}\}$$

$$\xrightarrow{280\ °C,\ Ir^{IV}\ reduction} NH_4^+\{Cr^{III}(NH_3)_{4-x}Cl_{1+x}\}\{Ir^{III}(NH_3)_xCl_{6-x}\}(x = 2-4)$$

$$\xrightarrow{400\ °C,\ further\ decomposition} \{Ir^{III}(NH_3)_{3-x}Cl_{5-x}\}\{Cr^{III}Cl_{1+x}\} + 1/6N_2 \uparrow + NH_4Cl + 2NH_{3(gas)};$$

$$(2)$$

$$[Ru^{III}(NH_3)_5Cl][Ir^{IV}Cl_6] \xrightarrow{280\ °C,\ ligand\ exchange} \{Ru^{III}(NH_3)_{5-x}Cl_{1+x}\}\{Ir^{IV}(NH_3)_xCl_{6-x}\}(x = 2-4)$$

$$(3)$$

$$\xrightarrow{280\ °C,\ Ir^{IV}\ reduction} NH_4^+\{Ru^{III}(NH_3)_{4-x}Cl_{1+x}\}\{Ir^{III}(NH_3)_xCl_{6-x}\} + 1/6N_{2(gas)}(x = 2-4);$$

$$[Rh^{III}(NH_3)_5Cl][Ir^{IV}Cl_6] \xrightarrow[stervise\ process]{367\ °C,\ ligand\ exchange} \{Rh^{III}(NH_3)_{5-x}Cl_{1+x}\}\{Ir^{IV}(NH_3)_xCl_{6-x}\}$$

$$(4)$$

$$\xrightarrow{367\ °C,\ Ir^{IV}\ reduction} NH_4^+\{Rh^{III}(NH_3)_{4-x}Cl_{1+x}\}\{Ir^{III}(NH_3)_xCl_{6-x}\} + 1/6N_{2(gas)};$$

$$[Ir^{III}(NH_3)_5Cl][Ir^{IV}Cl_6] \xrightarrow{375\ °C,\ ligand\ exchange} \{Ir^{III}(NH_3)_{5-x}Cl_{1+x}\}\{Ir^{IV}(NH_3)_xCl_{6-x}\}$$

$$(5)$$

$$\xrightarrow{375\ °C,\ Ir^{IV}\ reduction} NH_4^+\{Ir^{III}(NH_3)_{4-x}Cl_{1+x}\}\{Ir^{III}(NH_3)_xCl_{6-x}\} + 1/6N_{2(gas)}$$

It seems that it is quite common for Ir(IV) to form thermally unstable coordination compounds with a clear tendency to give Ir(III) species during their thermal treatment. Likely, a similar process will be detected in many other Ir(IV) species in the solid-state. The presence of the second metal in a high oxidation state, such as Co(III), results in a reduced stability of bimetallic salt in the solid-state as well as the presence of exothermic effects upon their thermal decomposition. In many previous works, polymeric structures with bridged ammonia or halogenide were proposed based on the stoichiometry of the intermediate products.[5–7] Nevertheless, only in several cases has it been proven spectroscopically. In the current study, the stability of octahedrally coordinated metals was proven. All early intermediates prepared below 300 °C do not have any lines in their Raman or IR spectra, which can be associated with the formation of ligand bridges. In other words, all intermediates have distorted octahedral coordination with nitrogen ligands preferably

decreases in the series: (**1**) > (**2**) > (**3**) > (**4**). (**5**) does not show any exothermal effects upon heating; only two corresponding overlapping endothermal effects can be detected in DSC. Ligand exchange and NH_3 to N_2 oxidation by metals are responsible for the thermal effects. In all salts, Ir(IV) to Ir(III) reduction is the main process which overlapped with Co(III) to Co(II) reduction in (**1**). $[M(NH_3)_5Cl][IrCl_6]$ with Cr(III), Ru(III), Rh(III) and Ir(III) cations do not transform into M(II) species which results in a much lower exothermal effect during decomposition. NH_3-ligands demonstrate a tendency to migrate to anionic Ir(III). After decomposition during the first step, cations and anions still have octahedral coordination and do not contain any bridged ligands. Mixed salts $[Ru_xIr_{1-x}(NH_3)_5Cl][IrCl_6]$ show a gradual decrease in the exothermic effect from pure (**3**) (maximal value) to $[Ru_{0.5}Ir_{0.5}(NH_3)_5Cl][IrCl_6]$, which is similar to (**5**) (no exothermic effect). Such findings can be used to tune the

thermodynamic properties and the stability of multimetallic compounds and single-source precursors.

Conflicts of interest

There are no conflicts to declare.

Acknowledgements

Notes and references

1 W. W. Wendlandt and J. P. Smith, *The Thermal Properties of Transition Metal Ammine Complexes*, Elsevier, Amsterdam-London-New York, 1967, p. 235.

2 B. Michelot, A. Ouali and M.-J. Blais, *et al.*, *New J. Chem.*, 1988, **12**, 293–298.

3 Yu. N. Kukushkin, V. F. Budanova and G. N. Sedova, *Solid-phase Thermal conversion of coordination compounds*, Leningrad State University, 1981, p. 176.

4 Yu. N. Kukushkin, V. F. Budanova and G. N. Sedova, *Russ. J. Inorg. Chem.*, 1980, **25**, 200.

5 L. D. Bolshakova, G. M. Larin, V. V. Minin, G. A. Zvereva, L. K. Shubochkin, Y. V. Rakitin and M. D. Valkovskii, *Russ. J. Inorg. Chem.*, 1992, **37**, 1542.

6 S. V. Korenev, S. V. Filatov, Yu. V. Shubin, A. N. Mikheev, S. A. Gromilov, A. B. Venediktov, V. N. Mit'kin and R. G. Kultyshev, *Russ. J. Inorg. Chem.*, 1996, **41**, 744.

7 T. I. Asanova, I. P. Asanov, M.-G. Kim, E. Yu. Gerasimov, A. V. Zadesenec, P. E. Plusnin and S. V. Korenev, *J. Nanopart. Res.*, 2013, **15**, 1994, DOI: 10.1007/s11051-013-1994-6.

8 S. A. Martynova, K. V. Yusenko, I. V. Korolkov, I. A. Baidina and S. V. Korenev, *J. Struct. Chem.*, 2009, **50**, 120, DOI: 10.1007/s10947-009-0016-0.

9 S. A. Gromilov, S. V. Korenev, I. A. Baidina, I. V. Korolkov and K. V. Yusenko, *J. Struct. Chem.*, 2002, **43**, 488.

10 S. A. Martynova, K. V. Yusenko, I. V. Korolkov and S. A. Gromilov, *Russ. J. Coord. Chem.*, 2007, **33**, 530.

11 K. V. Yusenko, S. A. Gromilov, I. A. Baidina, I. V. Korolkov and S. V. Korenev, *J. Struct. Chem.*, 2005, **46**, 109.

12 S. V. Korenev, A. B. Venediktov, Yu. V. Shubin, S. A. Gromilov and K. V. Yusenko, *J. Struct. Chem.*, 2003, **44**, 74.

13 D. I. Potemkin, E. Y. Semitut and Yu. V. Shubin, *et al.*, *Catal. Today*, 2014, **235**, 103–111.

14 S. A. Martynova, K. V. Yusenko, I. V. Korolkov and S. A. Gromilov, *Russ. J. Inorg. Chem.*, 2007, **52**, 1733.

15 S. V. Korenev, A. B. Venediktov, K. V. Yusenko and Yu. V. Shubin, *Russ. J. Coord. Chem.*, 2000, **26**, 358.

16 K. Nakamoto, *Infrared and Raman Spectra of Inorganic and Coordination Compounds, Theory and Applications in Inorganic Chemistry*, John Wiley, New Jersey, 6th edn, 2009, part A, p. 419.

17 M. Newville, *J. Synchrotron Radiat.*, 2001, **8**, 322.

18 K. V. Yusenko, S. Riva, P. A. Carvalho, M. V. Yusenko, S. Arnaboldi, A. S. Sukhikh, M. Hanfland and S. A. Gromilov, *Scr. Mater.*, 2017, **138**, 22.

19 K. Nakamoto, *Infrared and Raman Spectra of Inorganic and Coordinational Compounds, Applications in Coordination, Organometallic and Bioinorganic Chemistry*, John Wiley, New Jersey, 6th edn, 2009, part B, p. 408.

20 M. W. Bee, S. F. A. Kettle and D. B. Powell, *Spectrochim. Acta, Part A*, 1974, **30**, 139, DOI: 10.1016/0584-8539(74)80218-7.

21 B. Ravel and M. Newville, *J. Synchrotron Radiat.*, 2005, **12**, 537.

22 P. D. Bonnitcha, M. D. Hall, C. K. Underwood, G. J. Foran, M. Zhang, P. J. Beale and T. W. Hambley, *J. Inorg. Biochem.*, 2006, **100**, 963.

23 M. D. Hall, C. K. Underwood, T. W. Failes, G. J. Foran and T. W. Hambley, *Aust. J. Chem.*, 2007, **60**, 180.

24 A. Minguzzi, O. Lugaresi, E. Achilli, C. Locatelli, A. Vertova, P. Ghigna and S. Rondinini, *Chem. Sci.*, 2014, **5**, 3591.

25 Yu. V. Shubin, S. V. Korenev, K. V. Yusenko, T. M. Korda and A. B. Venediktov, *Russ. Chem. Bull.*, 2002, **51**, 41.

26 D. I. Potemkin, E. Yu. Filatov and A. V. Zadesenets, *et al.*, *Chem. Eng. J.*, 2012, **207–208**, 683.

27 P. Buchwalter, J. Rose and P. Braunstein, *Chem. Rev.*, 2015, **115**(1), 28.

28 M. Avisar-Levy, O. Levy, O. Ascarelli, I. Popov and A. Bino, *J. Alloys Compd.*, 2015, **635**, 48.